Submitted to IPMI 2005

Estimating the Statistics of Multi-Object Anatomic Geometry Using Inter-Object Relationships

Stephen M. Pizer, Ja-Yeon Jeong, Conglin Lu, Keith Muller, and Sarang Joshi

Medical Image Display & Analysis Group (MIDAG)
University of North Carolina, Chapel Hill NC 27599, USA

Abstract. We present a methodology for estimating the probability of multi-object anatomic complexes that reflects both the individual objects' variability and the variability of the inter-relationships between objects. The method is based on m-reps and the idea of augmenting medial atoms from one object's m-rep to the set of atoms of an object being described. We describe the training of these probabilities, and we present an example of calculating the statistics of the bladder, prostate, rectum complex in the male pelvis. Via examples from the real world and from Monte-Carlo simulation, we show that this means of representing multi-object statistics yields samples that are nearly geometrically proper and means and principal modes of variations that are intuitively reasonable.

1 Introduction

Since multiple objects form a given anatomic region, there has been a desire to characterize probabilistically populations of multi-object anatomic geometry. The approaches tried so far consist of representing the objects and doing global statistics on these representations, as derived from some dozens of training cases. Among the representations to which this approach has been applied are point distribution models [2], diffeomorphisms from atlases [**?**], distance functions or their levels sets [6], and our own m-reps [1]. We suggest that such global statistics pay inadequate attention to the objects themselves and most especially to the inter-relations among objects. We provide in this paper a method for generating probabilities directly on objects and their relationships. We show examples describing the variability of the bladder, prostate, and rectum complex in the male pelvis within a patient across a series of treatment days.

In other work of our laboratory [1] we have argued that for producing efficient models of anatomic geometry m-reps have advantages of representing object interiors and the local twisting, bending, displacements, and magnifications that regions of object interiors undergo. We have also argued that statistics on these nonlinear transformations need to be done using geodesic distance on the curved manifold of a symmetric space [3]. We adopt this representation and form of statistics in this paper. Also, in this paper we restrict the discussion to objects

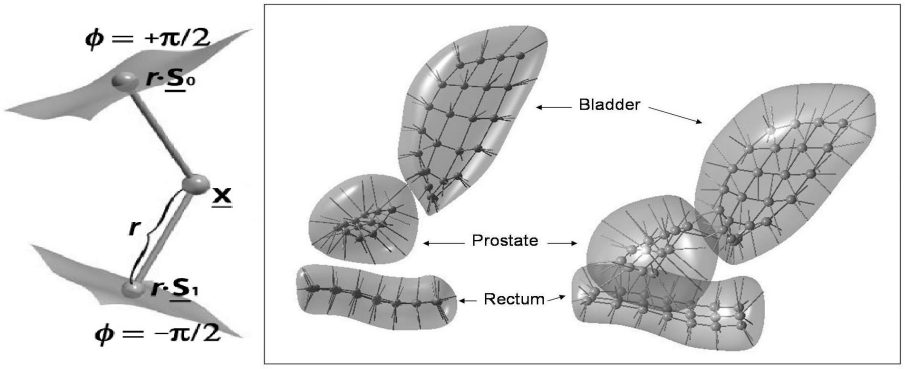

Fig. 1. Medial atom with a section of implied boundary surface (left). An m-rep 3-object complex for the bladder, the prostate, and the rectum of a patient in different view in a box (right).

each of which can be represented by a single sampled sheet of medial atoms (Fig. 1), i.e., "single-figure objects".

We begin from the assumption that we are given a single-figure m-rep model for multiple objects, for many training cases, and we assume further that the object complexes have already been aligned across the cases and that the medial atoms correspond across the cases.

We limit ourselves here to dealing with the information at the object level of locality. Thus, we assume that any truly global variation of the complex has been removed from each object, via the residue technique described in [4]. In addition, we do not treat here variations that are more local than at the object scale, despite the fact that our multiscale, coarse-to-fine approach described in [4] provides for additional analysis via the object cross-sections represented by medial atoms.

The subject of sections 2-6 is how to express and compute the probabilities of the objects and of the inter-object geometry. In section 2 we overview the approach and then in succession treat its three major components, namely section 3: atom augmentation to simultaneously capture objects and their relations to other objects, section 4: propagation of the inter-object relations to remaining objects and object parts, and section 5: inter-object residues to describe the variation remaining after the propagation of effects from other objects. In section 6 we explain how to train probabilities for objects by successive PGA's on object residues.

We say that a geometric model for a complex of non-interpenetrating objects is *proper* if a) the topology of the objects is retained, b) each object in the model does not have singularities or folds of its boundary or interior, and c) the non-interpenetration of objects is retained. Many previous methods for estimating inter-object probability distributions have produced samples some of

which are decidedly improper. In section 7 we test our method by illustrating that models sampled from our probability distributions on intra-patient bladder, prostate, and rectum deformations are nearly proper and that the means and principal modes of variation of these distributions are intuitively reasonable. We also briefly discuss application of these ideas to segmentation by posterior optimization. Section 8 discusses further opportunities for evaluation, and extensions and alternatives to the proposed methods.

2 Overview of the approach

We assume that in each case we have n objects, with m-reps $\{M_k\}_{k=1}^n$ where M_k can be taken as an ordered set of medial atoms. We remind the reader that each interior medial atom requires an 8-tuple to represent, describing a hub and two equal-length spokes (Fig. 1), and that each grid-edge medial atom requires a 9-tuple to represent, describing a hub, two equal-length spokes, and a third spoke formed from their bisector, which may be of a different length. In our present approach we assume that the objects will be provided in an order of decreasing stability, i.e., whose posterior probability, based on both geometric variability and intensity variability and edge sharpness, are in decreasing levels of tightness. In this work we will provide object statistics in this order, treating each object once. The details of dealing with these objects' statistics in sequence are described in section 6. In section 8 we discuss the extension to a form of a Markov process in which the method of iterative conditional modes is used, such that the objects are dealt with multiple times and if an object has another object as its neighbor, then the latter also has the former as a neighbor.

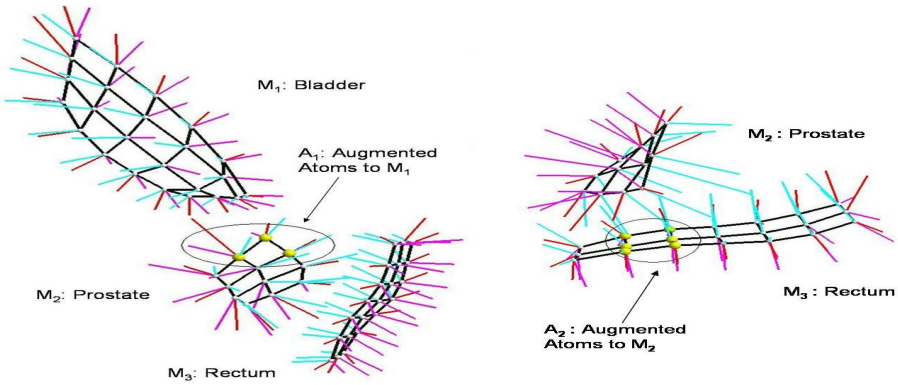

Fig. 2. A discrete m-rep for the bladder (M_1), the prostate (M_2), the rectum (M_3) 3-object complex of a patient. The augmented atoms in the prostate forming A_1 are shown with their hub enlarged (left). The prostate (M_2), the rectum (M_3) of the same patient the enlarged atoms in the rectum form A_2 (right).

The main new idea of this paper (Fig. 2) is that while estimating the statistics of a particular object M_k we deal with that object's inter-relation with other atoms by augmenting highly correlated atoms A_k in the remaining objects to M_k to produce representations $U_k = M_k \cup A_k$ whose statistics we study via principal geodesic analysis (PGA)[3]. PGA produces a mean and principal geodesic directions. This method of augmentation is discussed further in section 3.

The other aspect of our new idea is to propagate augmenting atoms' movement in the statistics of one augmented object to the remainder of the objects to be processed. The idea is that if an object changes position, pose, size, or shape, its neighboring objects will change sympathetically. In particular (Fig. 3), let all of the atoms in these other objects whose statistics are yet to be determined be R_k. The changes in A_k will be reflected in sympathetic changes in $R_k \setminus A_k$ [1] before the statistics on $R_k \setminus A_k$ are calculated. The details of this propagation are discussed in section 4.

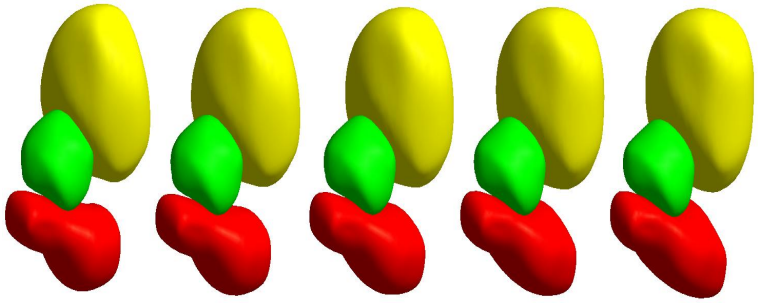

Fig. 3. Assuming we have produced statistics for the augmented bladder U_1, which has augmenting atoms A_1 in the prostate (M_2), we illustrate the sympathetic change of $R_1 \setminus A_1$ caused by A_1.

3 Objects inter-relation by augmentation

Because we have evidence that atoms in one object that are near another object are most highly correlated with that other object, we describe the inter-relation of a multi-object via these nearby atoms. In the male-pelvis example of Fig. 2, we expect that medial atoms in bladder M_1 be more highly correlated with medial atoms nearby in prostate A_1 than those in the rest of the prostate or in the rectum $R_1 \setminus A_1$. However, these atoms in the rest of the prostate and in the rectum atoms change their positions sympathetically as the medial mesh of the bladder enlarges. By augmenting the nearby prostate atoms forming A_1 to

[1] Recall that the notation $A \setminus B$ means the set difference A minus B.

those atoms in bladder to produce the representation of the augmented bladder U_1, we can study the effect of the deformation of the bladder on the augmenting atoms and then study the relation of changes in the augmenting atoms A_1 to that of rest of the prostate and the rectum, $R_1 \setminus A_1$. We use the latter results in a stage we call prediction, which is explained next.

4 Prediction of movements from augmentation by using the shape space of the remaining objects

In prediction we reflect a change in M_k in the statistics of R_k by predicting how $R_k \setminus A_k$ bends, twists or warps from the change of M_k through augmenting atoms A_k. In doing so, we take account of the shape space of the remainder objects R_k as suggested in [5], but using PGA in our a nonlinear symmetric space rather than the principal component analysis used in [5].

Recall that PGA involves first finding the mean μ of m-reps $\{\mathbf{M}_i \in \mathcal{M}\}_{i=1}^N$, where $\mathcal{M}$ is the symmetric space of an m-rep $\mathbf{M}_i$ and N is the number of training cases; projecting $\{\mathbf{M}_i\}_{i=1}^N$ to the tangent space $T_\mu\mathcal{M}$ at μ by the log map[2] ($\log_\mu : \mathcal{M} \to T_\mu\mathcal{M}$); and then doing PCA in the tangent space, which yields a set of principal directions $\{v_l\}_{l=1}^h$ in $T_\mu\mathcal{M}$. Taking the exponential map [3] ($\exp_\mu : T_\mu\mathcal{M} \to \mathcal{M}$) of $\{v_l\}_{l=1}^h$ gives a set of principal geodesics in $\mathcal{M}$, which in turn generates a submanifold $\mathcal{H}$ of $\mathcal{M}$. $\mathcal{H}$ is the shape space in which different modes of variations restricted to $\mathcal{H}$ of $\{\mathbf{M}_i\}_{i=1}^N$ are described via principal geodesics. The projection of $\mathbf{M}_i$ onto the shape space $\mathcal{H}$, $Proj_{\mathcal{H}}(\mathbf{M}_i)$[4], describes the unique variation within $\mathcal{H}$ nearest in geodesic distance to $\mathbf{M}_i$.

Now consider the augmented m-rep object $U_k = (M_k \cup A_k)$ and R_k ($A_k \subset R_k$). Let μ_r and H_r be the mean and the shape space generated by principal geodesics in the symmetric space $\mathcal{M}_r$ of R_k, which we can obtain by performing PGA on training cases of R_k. If we know how U_k deforms, i.e., how M_k and A_k change together, $Proj_{\mathcal{H}_r}(A_k)$ predicts how the remaining object R_k changes sympathetically through A_k in the shape space H_r:

$$Proj_{\mathcal{H}_r}(A_k) = \exp_{\mu_r}\left(\sum_{l=1}^{h_r}\langle \log_{\mu_r}(A_k), v_l\rangle \cdot v_l\right), \tag{1}$$

where $\{v_l\}_{l=1}^{h_r}$ are principal directions in the tangent space of μ_r corresponding to the principal geodesics in H_r and the dimension of $\log_{\mu_r}(A_k)$ is adjusted to match with that of v_l by adding zeros to $\log_{\mu_r}(A_k)$ for parameters corresponding to $R_k \setminus A_k$. Then the prediction for the remainder R_k can be defined as

$$Pred(R_k;\, A_k) := Proj_{\mathcal{H}_r}(A_k)\ . \tag{2}$$

Notice that $Pred(R_k;\, A_k)$ is also an m-rep.

[2] Refer to [3] for detailed explanation of log map.

[3] Refer to [3] for detailed explanation of exponential map.

[4] More precisely, the projection operator $Proj_{\mathcal{H}} : \mathcal{M} \to \mathcal{H}$ is approximated by $Proj_{\mathcal{H}}(\mathcal{M}) = \exp_\mu\left(\sum_{l=1}^{h}\langle \log_\mu(\mathcal{M}), v_l\rangle \cdot vl\right)$. For detailed explanation, refer to [3].

5 Residues of objects in order

If we describe the changes in U_k and the sympathetic changes in $R_k \setminus A_k$, all that is left to describe statistically is the remaining changes in R_k after the sympathetic changes have been removed. If the objects are treated in order and each object has augmenting atoms only in the next object, this will mean that n probability distributions will need to be trained, namely, for U_1, for U_2 after the sympathetic changes from U_1 have been removed, for U_3 after the sympathetic changes from U_1 and U_2 have been removed, ... , for U_n after the sympathetic changes from $U_1, U_2 \ldots$, and U_{n-1} have been removed. The removal of sympathetic changes is accomplished via the residue idea described in [4]. Next we explain how such residues are applied between a predicted remainder $\mathcal{N}^0$ and the actual value $\mathcal{M}$ of that remainder.

5.1 Difference of medial atoms

A medial atom $\mathbf{m} = (\mathbf{x},\, r,\, \mathbf{u}, \mathbf{v})$ is defined as an element of the symmetric space $G = R^3 \times R^+ \times S^2 \times S^2$ where the position $\mathbf{x} \in R^3$, the spoke length $r \in R^+$, and two unit spoke directions $\mathbf{u}, \mathbf{v} \in S^2$ (S^2 is a unit sphere). If an m-rep has d medial atoms, the m-rep parameter space becomes $\mathcal{M} = G^d$. Let $\mathbf{R_w}$ represent the rotation along the geodesics in S^2 that moves a point $\mathbf{w} \in S^2$ to the north pole $\mathbf{p} = (0, 0, 1) \in S^2$. For given any two medial atoms $\mathbf{m}_1, \mathbf{m}_2 \in G$ where $\mathbf{m}_i = (\mathbf{x}_i,\, r_i,\, \mathbf{u}_i, \mathbf{v}_i)$, $i = 1, 2$, the difference between them can be described as follows:

$$\begin{gathered} \ominus : G \times G \longrightarrow G \\ \mathbf{m}_1 \ominus \mathbf{m}_2 := (\mathbf{x}_1 - \mathbf{x}_2,\, \tfrac{r_1}{r_2},\, \mathbf{R}_{\mathbf{u}_2}(\mathbf{u}_1)\, \mathbf{R}_{\mathbf{v}_2}(\mathbf{v}_1)) \ . \end{gathered} \tag{3}$$

$\mathbf{m}_1 \ominus \mathbf{m}_2$ is the difference between $\mathbf{m}_1, \mathbf{m}_2$ relative to $\mathbf{m}_2$ coordinates. Like $\mathbf{m}_1$ and $\mathbf{m}_2$, $\mathbf{m}_1 \ominus \mathbf{m}_2 \in G$.

Corresponding to the difference operator $\ominus$, the addition operator $\oplus$ can be defined as:

$$\begin{gathered} \oplus : G \times G \longrightarrow G \\ \mathbf{m} \oplus \Delta\mathbf{m} := (\mathbf{x}_1 + \mathbf{x}_2,\, r \cdot \Delta r,\, \mathbf{R}_{\mathbf{u}}^{-1}(\Delta\mathbf{u}),\, \mathbf{R}_{\mathbf{v}}^{-1}(\Delta\mathbf{v})) \end{gathered} \tag{4}$$

for given $\mathbf{m} = (\mathbf{x},\, r,\, \mathbf{u}, \mathbf{v})$ and the difference $\Delta\mathbf{m} = (\Delta\mathbf{x},\, \Delta r,\, \Delta\mathbf{u}, \Delta\mathbf{v})$. This operation is neither commutative nor associative. As an m-rep object is a collection of medial atoms, these operations can be individually applied to each atom of the object.

5.2 Residues in object stage

Our probabilistic analysis proceeds object by object in order. After some object has been described probabilistically and its sympathetic effect has been applied to its remainder, there is a further change in the remaining objects to be described. We call that further change the residue of the remainder objects with respect to the probability distribution on the first. More precisely, let $\mathbf{M} \in \mathcal{M}$

be an m-rep or an m-rep residue of one object fitting a particular training case where $\mathcal{M}$ is a symmetric space of $\mathbf{M}$ and let $p(\mathbf{N})$ be a probability distribution on $\mathbf{N} \in \mathcal{M}$ describing part of the variation of $\mathbf{M}$. Notice that if $D(p)$ represents the domain of p, then $D(p)$ is a submanifold of $\mathcal{M}$. Relative to the probability distribution p, $\mathbf{N}^0$, the closest m-rep to $\mathbf{M}$ in $D(p)$, is

$$\mathbf{N}^0 = \arg \min_{\mathbf{N} \in D(p)} d(\mathbf{M}, \mathbf{N}), \tag{5}$$

where $d(\mathbf{M}, \mathbf{N})$ is the geodesic distance on $\mathcal{M}$. Then the residue $\Delta\mathbf{M}$ of $\mathbf{M}$ with respect to p can be defined as

$$\Delta\mathbf{M} := \mathbf{M} \ominus \mathbf{N}^0 \ . \tag{6}$$

In the method we are describing, we use the prediction $Pred(\mathbf{M}; \mathbf{A})$ from a set of augmented atoms $\mathbf{A}$ in $\mathbf{M}$ to $\mathbf{M}$'s previous object (of which movements have an effect on $\mathbf{M}$) as an approximation to $\mathbf{N}^0$ because the prediction is made on the shape space of $\mathbf{M}$ and the augmentation can give a good estimation to the overall effect of $\mathbf{M}$'s previous object. We expect the prediction $Pred(\mathbf{M}; \mathbf{A})$ to be close to $\mathbf{N}^0$. Thus we compute $\Delta\mathbf{M} := \mathbf{M} \ominus Pred(\mathbf{M}; \mathbf{A})$.

6 Training the probabilities for objects

Training the probabilities for the object is done via successive PGA's on the object residues. Let $O_i^r = \{M_{jk}^r\}_{k \in J}$ be the i^{th} training case of a multi-object m-rep residue for $i \in I$, where $I = \{1, \ldots, N\}, J = \{1, \ldots, n\}$ are index sets for N training cases and n objects. As mentioned in Sec. 1, O_i^r is a multi-object m-rep residue from which any truly global variations are removed from $\{M_{ik}\}_{k \in J}$.

The residue $\{O_i^r\}_{i \in I}$ are treated in the order of objects M_k from $k = 1$ to n. First we apply PGA on $\{U_{i1}^r\}_{i \in I}$, the residue of the first object, to get the mean μ^1 and a set of principal variances and associated principal geodesics $\{\exp_{\mu^1}(v_l^1)\}_{l=1}^{n_1}$, where $v_l^1 \in T_{\mu^1}\mathcal{M}^1$. This mean, principal variances, and principal geodesics provide our estimate of the probability distribution of U_1^r. Let $\mathcal{H}^1$ be a submanifold of $\mathcal{M}^1$ where $\mathcal{M}^1$ is the symmetric space for U_1^r. The projection of U_{i1}^r of i^{th} case onto the geodesic submanifold $\mathcal{H}^1$, $Proj_{\mathcal{H}^1}(U_{i1}^r)$, describes the variation unique to U_{i1} in H^1. Now we need to update the residue $\{R_{i1}^r\}_{i \in J}$ to reflect the sympathetic effect from M_1^r on R_1^r by A_1^r. That is done by the prediction $Pred(R_{i1}^r;\ A_{i1}^r)$ as described in Sec. 4.

So the residue for the next object (the second object) that we use to apply PGA is no longer $\{O_i^r\}_{i \in I}$. The updated residue of the remainder to the first object becomes

$$R_{i1}^{r1} = R_{i1}^r \ominus Pred(R_{i1};\ A_{i1}) \qquad i \in I \ . \tag{7}$$

Once we have the new updated residue $U_{ik}^{r(k-1)} \subset R_{ik}^{r(k-1)}$ for the k^{th} object, $k = 2, \ldots, n$, we repeat the same steps 1) applying PGA on $U_{ik}^{r(k-1)}$ and 2) updating the residue of the remainder, which produces a set of means $\{\mu^k\}_{k \in J}$ and sets of principal geodesics $\{\{\exp_{\mu^k}(v_l^k)\}_{l=1}^{n_k}\}_{k \in J}$ on object residues.

7 Geometrically proper objects in probability distributions in the male pelvis

Samples being geometrically improper has been a problem for other methods such as PCA on distance functions or on dense PDMs. Examples of what we mean by geometrically improper is wrong topology, interpenetration of separated objects, folding, and singularities such as unwanted corners and cusps. There are two reasons why we would expect that our methods would avoid geometrically improper samples from their probability distributions.

1) M-reps are founded on the idea that using primitive transformations including local twisting and bending of object interiors will yield an economical representation of the single and multi-object transformations of anatomy between individuals or within an individual over time. When using such rotational transformations in the representation methods and in particular in the methods of description of object inter-relations via augmentation and prediction, nonlinear PGA is necessary to produce sample object complexes that are geometrically proper.

2) The regular grids of medial atoms that we generate from training binary images of objects [8] are designed to have large geodesic distance to improper entities on the manifold $\mathcal{M}$. Thus we might hope that objects within $[-2, +2]$ standard deviations will also be proper. Analysis of our objects using a criterion based on the radial shape operator of [7] could be used to avoid improper models, but this criterion has not been applied in the work described in this paper.

The most basic test of our probability distributions is to visually judge whether those generated samples are proper and whether the principal geodesic directions derived from real patient data explain variations we see in the training samples.

Because our training set is just a particular sample subset of a population of m-reps, we wish to know how our method would fare on other training sample subsets. We can accomplish this by generating new random samples from our probability distributions and test whether training from these samples produces a probability distribution whose samples are proper.

We generate the new samples by assuming that each tangent plane principal component from the original training follows the standard normal distribution once we scale the principal directions by the square root of corresponding eigenvalues in the tangent space. Thus, for each object residue we randomly sample each principal component following the standard normal distribution to generate random points on each tangent space about the mean $\{\mu^k\}_{k\in J}$. By taking exponential maps of those points, we generate m-reps and residues that can be combined by $\oplus$ to produce new training sample m-reps. PGA on such a new sampled training set yields a new mean and set of principal directions and variances, whose samples we can judge as to how proper they are.

We applied our new method to obtain the probability distributions from two training sets, each of which are obtained from bone-aligned male-pelvis CT images of a real patient over several days. A single-figure m-rep was fit to each organ: 4x6 grids of medial atoms for the bladder, 3x4 grids for the prostate,

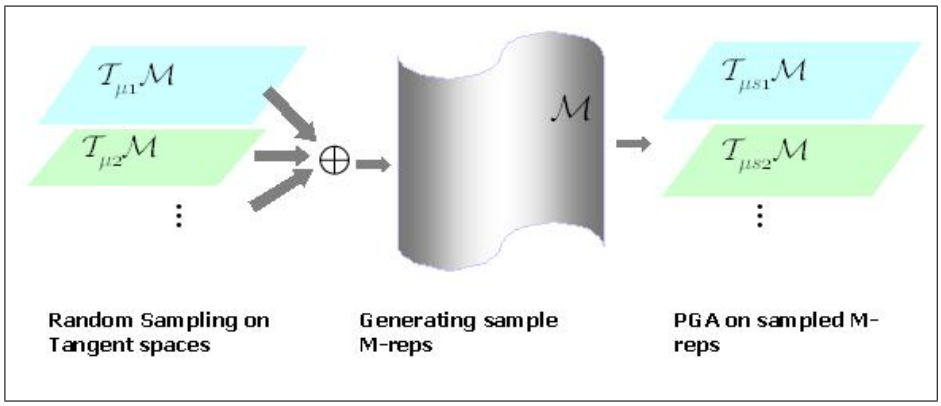

Fig. 4. Left: tangent spaces at object residue means from real patient data. Middle: m-rep parameter space. Right: object residue means from generated training data. Click the figure to see the movies of 100 sampled m-reps from patient 1 data and from patient 2 data. In the movie the point of view changes from time to time.

and 3x7 grids for the rectum. The total number of medial atoms is 57, so the dimension of the m-rep parameter space is 456. Our software to fit the single figure m-reps to binary image of each organ provides reasonable correspondence of medial atoms across cases by penalizing irregularity and rewarding correspondence to one case [8]. Inter-penetrations among m-reps of the three objects were prevented in the fitting [8] of each training case. We have 12 cases (m-reps) of one patient (patient 1) and 17 cases of another patient (patient 2).

Figure. 5 displays the first modes of variation of patient 1 and 2 at PGA coefficients -3, -1.5, 1.5, 3 standard deviations of bladder with prediction, prostate with prediction and rectum in Fig. 5 from the top row to the bottom row.

In these movies, as well as the ones seen in fig. 4, we see the following behaviors:

- The m-reps produced as samples or chosen along principal geodesics yield very limited inter-object penetration, as desired since none of the training samples have inter-object penetration.
- The surfaces of the m-rep sample implied objects are smooth, with few exceptions. Folding is not observed, and the introduction of sharp ridges happens seldom, only at crest positions which are sharp in some of the training cases.
- The principal geodesics seem to correspond to anatomically observed changes. For example, we see strong growth in the bladder corresponding to filling and strong bulging of the rectum corresponding to the introduction of bowel gas. In contrast, the prostate residue shows only modest shape changes, a behavior expected from the fact that the prostate is typically quite hard.

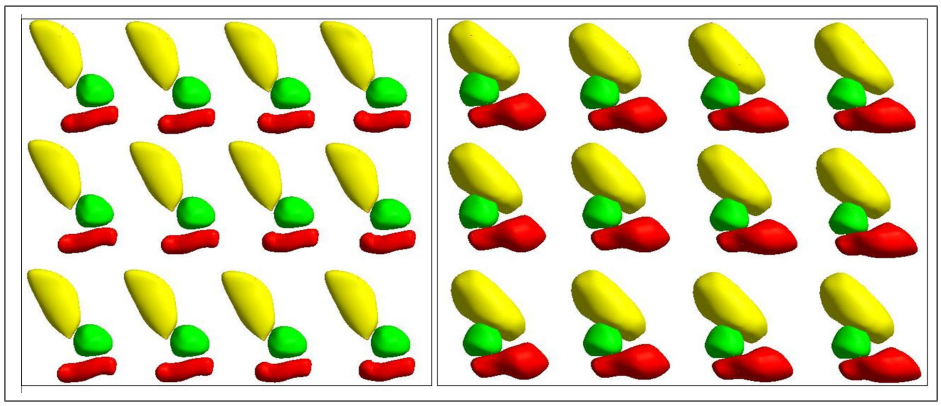

Fig. 5. Illustration of first modes of variation of patient 2 in the box on the left and that of patient 1 in the box on the right. Click the figure to see the first modes of variations of first patient 2 and then patient 1.

It is in this sense that we say that our statistical method provides samples that are "nearly geometrically proper and means and principal modes of variations that are intuitively reasonable."

In addition to the evaluation of m-rep probabilities just described, we can also judge the probabilities by their usefulness as a prior in segmentation by posterior optimization of m-reps of the bladder, prostate, rectum complex in new target images of the same patient on different days. The details of this segmentation approach are given in [4], [10], and the results on a few cases, agreeing well with human segmentations, have been reported in [11].

8 Discussion and Conclusion

We presented new ideas in estimating the probability distribution of multi-object anatomic objects via augmentation and prediction with principal geodesic analysis suggested in [3]. We can apply our approach to get statistics of multi-figure objects of m-reps: taking hinge atoms as augmented atoms and predicting the sympathetic change of a subfigure from the change of its host figure. [9] explains the multi-figure structure of m-rep objects and its application to anatomical objects. In this paper, we have limited the residue to the object level of locality. But we can compute finer residues at the medial atom level of locality and do further analysis as described in [4].

Other evaluations of the sample probability distributions generated using Monte Carlo approaches to generate new sample training sets are in progress. These involve measuring the bias and reliability of the resulting probability distributions.

There are some issues that we need to address in our approach: the order of objects in applying PGA to object residues, the choice of augmented atoms, and the neighbor relation between objects. Firstly, while in this paper we assume that objects with less variation are handled first and objects with more variation are handled later, we have not truly measured the amounts of variation to make this judgment. It remains for us to find a means of doing that.

Alternatively, we can avoid ordering the objects by considering the mutual neighbor relation in augmentation. This extension from the present approach is suggested by real situations such as male-pelvis example that we used: not only can the bladder induce a change in the prostate and rectum but also the change of a prostate can induce sympathetic change in the bladder and rectum, etc. This suggests a Markov random field model on neighboring objects, and thus an Iterative Conditional Modes algorithm alternating among the which is the primary object being deformed and which are the remainder undergoing sympathetic changes.

Secondly, we choose the augmented atoms based on the distance between atoms in one object and the other because we have preliminary evidence done by [4] that those nearby atoms are highly correlated. Another test needed is whether the remaining atoms are independent of the primary object when conditioned on the augmenting atoms.

Finally, a possible measure to explain the inter-object relation is to use canonical correlation. A canonical correlation is the correlation of two sets of canonical variables, one set representing independent variables and the other set dependent variables. The purpose of canonical correlation is to explain the relation of the two sets of variables. For each canonical variable, we can also assess how strongly it is related to measured variables in its own set, or the set for the other canonical variable. We speculate that we can incorporate this canonical correlation on the curved manifold space of m-reps as an alternative to the method described in this paper.

References

1. S.M. Pizer, T. Fletcher, Y. Fridman, D.S. Fritsch, A.G. Gash, J.M. Glotzer, S. Joshi, A. Thall, G Tracton, P. Yushkevich, and E.L. Chaney, "Deformable M-Reps for 3D Medical Image Segmentation," *International Journal of Computer Vision* - Special UNC-MIDAG issue, (O Faugeras, K Ikeuchi, and J Ponce, eds.), vol. 55, no. 2, pp. 85-106, Kluwer Academic, November-December 2003
2. T.F. Cootes, C.J. Taylor, D.H. Cooper, and J. Graham, "Active Shape Models Their Training and Application," *Computer Vision and Image Understanding*, Elsevier, Vol. 61 (1995), No. 1, pp.38-59.
3. P.T. Fletcher, C. Lu, S.M. Pizer, and S. Joshi, "Principal Geodesic Analysis for the Study of Nonlinear Statistics of Shape," *IEEE Transactions on Medical Imaging*, vol. 23, no. 8, pp. 995-1005, IEEE, Aug. 2004.
4. C. Lu, S.M. Pizer, and S. Joshi, "Statistical Multi-object Shape Models," *in preparation.*

5. K. Rajamani, S.C. Joshi, and M. Styner, "Bone model morphing for enhanced surgical visualization," in *International Symposium on Biomedical Imaging*, pp.1255-1258, Apr. 2004.
6. A. Tsai, A. Yezzi, W. Wells, C. Tempany, D. Tucker, A. Fan, E. Grimson, A. Willsky, "A Shape-Based Approach to Curve Evolution for Segmentation of Medical Imagery," *IEEE Transactions on Medical Imaging*, Vol. 22, No. 2, 137-154, February 2003.
7. J. Damon, "Determining the Geometry of Boundaries of Objects from Medial Data," To appear, *International Journal of Computer Vision*, 2004.
8. D. Merck, S. Joshi, G. Tracton, S.M. Pizer, "On Single Figure Statistical M-Rep Model Construction," *in preparation*.
9. Q. Han, C. Lu, G. Liu, S.M. Pizer, S. Joshi, and A. Thall, "Representing Multi-Figure Anatomical Objects," in *International Symposium on Biomedical Imaging*, pp. 1251-1254, Apr. 2004.
10. S.M. Pizer, P.T. Fletcher, S. Joshi, A.G. Gash, J. Stough, A. Thall, G. Tracton, and E.L. Chaney, "A Method and Software for Segmentation of Anatomic Object Ensembles by Deformable M-Reps," To appear, *Medical Physics*, no. , 2005.
11. E. Chaney, S.M. Pizer, S. Joshi, R. Broadhurst, P.T. Fletcher, G. Gash, Q. Han, JY. Jeong, C. Lu, D. Merck, J. Stough, G. Tracton, MD J. Bechtel, J. Rosenman, YY. Chi, and K. Muller. "Automatic Male Pelvis Segmentation from CT Images via Statistically Trained Multi-Object Deformable M-rep Models," *Presented at American Society for Therapeutic Radiology and Oncology* , 2004.